Biomaterials Translational

Microarray analysis of signalling interactions between inflammation and angiogenesis in subchondral bone in temporomandibular joint osteoarthritis

Wenpin Qin[1,#], Jialu Gao[1,#], Jianfei Yan[1,#], Xiaoxiao Han[1], Weicheng Lu[1], Zhangyu Ma[1], Lina Niu[2], Kai Jiao[1,]*

Key Words:
angiogenesis; inflammation; osteoarthritic pain; osteoarthritis; subchondral bone; temporomandibular joint (TMJ)

From the Contents

Introduction	175
Methods	176
Results	177
Discussion	179

ABSTRACT

Inflammation and angiogenesis, the major pathological changes of osteoarthritis (OA), are closely associated with joint pain; however, pertinent signalling interactions within subchondral bone of osteoarthritic joints and potential contribution to the peripheral origin of OA pain remain to be elucidated. Herein we developed a unilateral anterior crossbite mouse model with osteoarthritic changes in the temporomandibular joint. Microarray-based transcriptome analysis, besides quantitative real-time polymerase chain reaction, was performed to identify differentially expressed genes (DEGs). Overall, 182 DEGs (fold change ≥ 2, $P < 0.05$) were identified between the control and unilateral anterior crossbite groups: 168 were upregulated and 14 were downregulated. On subjecting significant DEGs to enrichment analyses, inflammation and angiogenesis were identified as the most affected. Inflammation-related DEGs were mainly enriched in T cell activation and differentiation and in the mammalian target of rapamycin/nuclear factor-κB/tumour necrosis factor signalling. Furthermore, angiogenesis-related DEGs were mainly enriched in the Gene Ontology terms angiogenesis regulation and vasculature development and in the KEGG pathways of phosphoinositide 3-kinase-protein kinase B/vascular endothelial growth factor/hypoxia-inducible factor 1 signalling. Protein–protein interaction analysis revealed a close interaction between inflammation- and angiogenesis-related DEGs, suggesting that phosphatidylinositol-4,5-bisphosphate 3-kinase catalytic subunit delta (Pi3kcd), cathelicidin antimicrobial peptide (Camp), C-X-C motif chemokine receptor 4 (Cxcr4), and MYB proto-oncogene transcription factor (Myb) play a central role in their interaction. To summarize, our findings reveal that in subchondral bone of osteoarthritic joints, signal interaction is interrelated between inflammation and angiogenesis and associated with the peripheral origin of OA pain; moreover, our data highlight potential targets for the inhibition of OA pain.

http://doi.org/10.12336/biomatertransl.2024.02.007

How to cite this article:
Qin, W.; Gao, J.; Yan, J.; Han, Xi.; Lu, W.; Ma, Z.; Niu, L.; Jiao, K. Microarray analysis of signalling interactions between inflammation and angiogenesis in subchondral bone in temporomandibular joint osteoarthritis. *Biomater Transl.* **2024**, *5*(2), 175-184.

Introduction

Osteoarthritis (OA), a prevalent disease worldwide, is a major cause of discomfort and disability, significantly impacting the quality of life of more than 500 million people.[1] With increasing life expectancy, OA incidence escalates, posing significant societal and healthcare burdens. OA is a multifaceted joint pathology affecting diverse articular tissues, including cartilage, subchondral bone, and synovium, among others. When OA patients seek treatment, joint pain is the principal concern and a leading contributor to functional decline and disability. Pain management in OA remains elusive due to incomplete understanding of its mechanisms. Current therapies, such as non-steroidal anti-inflammatory drugs, analgesics, and steroids, frequently fall short in providing lasting pain relief and carry notable adverse effects, underscoring the complexity of the pathophysiology of OA pain.[2]

Both the central and peripheral nervous systems have been verified to participate in OA.[3] The central mechanisms of OA pain include central sensitisation coupled with aberrant modulation of ascending and descending neural pathways originating in the brain.[4] Pharmacological interventions often target central pain mechanisms for symptom relief, but current treatments are often limited by potential adverse events. The peripheral mechanisms of OA pain have recently attracted much interest. Synovial inflammation has been reported to cause OA pain by increasing the responsiveness of peripheral nociceptive neurons.[5] Notably, OA pain can manifest at very early stages of the disease in the absence of synovial inflammation, but the changes at subchondral bone are present.[6] At present, the peripheral triggers of OA pain, particularly in the early stage of the disease, are unclear.

Early-stage OA is characterised by aberrant subchondral bone remodelling, a process increasingly recognized as a key driver of OA pathology. Lesions occurring in subchondral bone, including oedema-like lesions, show a close relationship with the intensity of pain in patients with OA.[7] Some agents (e.g., zoledronic acid) are able to target oedema-like lesions in subchondral bone, resulting in obvious pain relief.[8] Furthermore, after knee replacement, once the deteriorated subchondral bone with overlying cartilage is removed, pain is alleviated.[9] It has been suggested that abnormal subchondral bone remodelling, including inflammation, angiogenesis, and innervation, plays a key role in the origin of OA pain.[10] Immunocytes infiltrating subchondral bone of osteoarthritic joints secrete diverse inflammatory mediators, such as prostaglandin E and transforming growth factor-β,[11] which play vital pro-pathogenic roles in OA pathogenesis. Peripheral sensory neurons bear receptors for diverse inflammatory molecules, whose activation heightens pain sensitivity by engaging secondary messengers that augment neuronal excitability, thereby directly contributing to pain. For example, it has been reported that the inflammation mediator prostaglandin E mediates angiogenesis and innervation in subchondral bone of mice with OA, promoting OA progression and pain.[12] In addition, angiogenesis, which is closely integrated with the process of neurogenesis, facilitates immunocyte infiltration and contributes to pain. Therefore, a better understanding of signalling interactions underlying the pathogenesis of subchondral bone of osteoarthritic joints, particularly that related to inflammation and angiogenesis, is urgently needed to develop disease-modifying therapy for OA pain.

The temporomandibular joint (TMJ), vital to dental occlusion, is frequently susceptible to occlusal disruptions that can instigate OA.[13] We developed a TMJ OA mouse model by abnormal dental occlusion, referred to as unilateral anterior crossbite (UAC) model.[14] An association has been found between abnormal subchondral bone remodelling and increased angiogenesis and innervation at the osteochondral interface.[15] Our study utilised microarray transcriptomics to pinpoint genes linked to inflammation, angiogenesis, and innervation. Enrichment and protein–protein interaction (PPI) analyses refined the identification of significant differentially expressed genes (DEGs). We hypothesised that signal transduction is interrelated between inflammation and angiogenesis in osteoarthritic subchondral bone and associated with the peripheral origin of OA pain.

Methods

TMJ OA mouse model

Sixteen C57BL/6 mice (8-week-old, female, weight 20–30 g) were provided by the Animal Centre of the Air Force Medical University (AFMU) (Xi'an, China; licence No. SYXK (Shaan) 2019-001). Given the heightened susceptibility of females to TMJ arthritis, this study exclusively utilized female mice.[16] All animal experiments were performed in accordance with the National Institute of Health Guidelines for the Care and Use of Laboratory Animals and approved by the Institutional Animal Care and Use Committee of AFMU (approval No. IACUC-20241298; approved on February 20, 2023). Mice were randomized into UAC and control groups (n = 8/group). The UAC group underwent attachment of a metallic UAC appliance (fabrication of UAC appliance using 18G needles obtained from Shuguang Jianshi, Luohe, China) to the left lower incisors, as previously described.[14] The mice in the Control group underwent a mock surgery; no UAC appliances were attached.

Histology and immunofluorescence staining

Three weeks after model, all mice were euthanised through an intraperitoneal administration of an overdose of pentobarbital. No differences were present in degradative changes between the left and right sides of the same TMJ mouse. The condyles were examined via micro-computed tomography (Inveon, Siemens AG, Munich, Germany) scanning with a defined resolution of 8 μm. Then, left condylar tissue specimens underwent fixation in 4% paraformaldehyde, followed by decalcification in 10% ethylenediamine tetra-acetic acid, and subsequent paraffin embedding for histological preparation. Subsequently, 5-μm central sagittal sections were sectioned and processed for histological examination with haematoxylin-eosin, safranin O/fast green staining to assess cartilage morphology, and immunofluorescence staining to detect specific protein expression patterns. The right condylar subchondral bone was harvested for quantitative polymerase chain reaction (qPCR). The tissue sections, adhered to poly-L-lysine-coated glass slides, were thoroughly deparaffinised. A portion of

1 Department of Stomatology, Tangdu Hospital & State Key Laboratory of Oral and Maxillofacial Reconstruction and Regeneration & School of Stomatology, The Fourth Military Medical University, Xi'an, Shaanxi Province, China; 2 State Key Laboratory of Oral and Maxillofacial Reconstruction and Regeneration & National Clinical Research Centre for Oral Diseases & Shaanxi Key Laboratory of Stomatology, School of Stomatology, The Fourth Military Medical University, Xi'an, Shaanxi Province, China

*Corresponding author: Kai Jiao, kjiao1@163.com.

#Author equally.

these sections were subjected to standard haematoxylin-eosin staining protocol (Solarbio Science & Technology Co., Ltd., Beijing, China). In preparation for safranin O/fast green (Solarbio Science & Technology Co., Ltd.) histological analysis, sections were initially stained with 0.02% fast green to visualise collagen, followed by 0.1% safranin O infiltration to highlight proteoglycan content within the extracellular matrix, thus enabling detailed assessment of tissue structure and composition. Images were captured using an optical microscope (Leica Microsystems, Wetzlar, Germany). Bone histomorphometry was performed on the subchondral bone of HE-stained sections as previously reported,[17] by Adobe Photoshop 2021 (Adobe Systems, San Jose, CA, USA). The chosen histomorphometric parameter was bone volume fraction (bone volume (BV)/tissue volume (TV)) = bone area/tissue area.

To conduct immunofluorescence staining, the protocol entailed sequential deparaffinisation, rehydration, and inhibition of endogenous peroxidase activity. Subsequently, specimens were immersed in 5% goat serum (MilliporeSigma, Burlington, MA, USA) or donkey serum (SL050, Solarbio Science & Technology Co., Ltd.) to block unspecific epitopes.

Specimens were subjected to sequential incubations: initially with primary antibodies against calcitonin gene-related peptide (CGRP; goat, 1:200, Abcam, Cambridge, UK, Cat# ab36001, RRID: AB_725807), CD31 (mouse, 1:200, Santa Cruz Biotechnology, Dallas, TX, USA, Cat# sc-376764, RRID: AB_2801330), or CD4 (rabbit, 1:200, Abcam, Cat# ab183685, RRID: AB_2686917) at 4°C overnight and subsequently with a fluorochrome-labelled secondary antibodies (Goat Anti-Rabbit IgG H&L (Alexa Fluor® 594), 1:200, Abcam, Cat# ab150080, RRID: AB_2650602; Goat Anti-Mouse IgG H&L (Alexa Fluor® 594), 1:200, Abcam, Cat# ab150116, RRID: AB_2650601; Donkey Anti-Goat IgG H&L (Alexa Fluor® 594), 1:200, Abcam, Cat# ab150132, RRID: AB_2810222) for 2 hours at room temperature. Following thorough rinsing with phosphate buffered saline, slides were coverslipped using Prolong Diamond Antifade Mountant containing 4′,6-diamidino-2-phenylindole (Invitrogen, San Diego, CA, USA) for nuclear staining. High-resolution immunofluorescence images were acquired using a FV1000 Laser Scanning Confocal Microscope (Olympus, Tokyo, Japan) and meticulously analysed with the ImageJ 2 (National Institutes of Health, Bethesda, MD, USA),[18] facilitating precise qualitative and quantitative evaluations of markers.

Microarray

Subchondral bone tissues of the condyle were delicately pulverized in an environment of liquid nitrogen to preserve RNA integrity. Thereafter, the isolation and purification of total RNA were methodically conducted utilizing TRIzol reagent and RNeasy Mini Kit (Qiagen, Hilden, Germany), in strict adherence to the manufacturers' instructions. Each sample underwent rigorous on-column DNase digestion to eliminate genomic DNA contamination. RNA samples, post-reverse transcription to complementary DNA and Cy3 labeling with Agilent's Quick Amp Kit (Agilent Technologies, Santa Clara, CA, USA), were equilibrated by concentration and subjected to hybridisation on Whole Mouse Genome Microarrays (4 × 44K; Agilent Technologies). Scanned with a G2505C microarray scanner (Agilent), signal intensities were processed by Feature Extraction 9.5.3 and analysed in GeneSpring GX10 software (Agilent) for normalisation and profiling. Genes meeting criteria of fold change ≥ 2 and $P \leq 0.05$ were onsidered as DEGs. The R language's limma and Bioconductor packages were used for correlation analysis between different samples.

To elucidate functional roles and pathways, the Database for Annotation, Visualisation, and Integrated Discovery (DAVID; Laboratory of Immunopathogenesis and Bioinformatics, SAIC, Frederick, Inc., Frederick, MD, USA; https://david.ncifcrf.gov/) was employed for comprehensive Gene Ontology (GO) and Kyoto Encyclopedia of Genes and Genomes (KEGG) enrichment analyses.[18] PPI networks were meticulously constructed using the Search Tool for the Retrieval of Interacting Genes/Proteins (STRING; available at https://string-db.org/)[19] and visualised with CytoScape software, version 3.9.0 (Institute of Systems Biology, Seattle, WA, USA, accessible at https://cytoscape.org/).[20]

qPCR

qPCR was performed as previously described.[21, 22] The expression levels of phosphatidylinositol-4,5-bisphosphate 3-kinase catalytic subunit delta (*Pi3kcd*), cathelicidin antimicrobial peptide (*Camp*), C-X-C motif chemokine receptor 4 (*Cxcr4*), and MYB proto-oncogene transcription factor (*Myb*) were determined to validate microarray results. Glyceraldehyde-3-phosphate dehydrogenase (*Gapdh*) served as the internal control gene. Primer sequences are detailed in **Additional Table 1**. Quantitative analysis was undertaken by $2^{-\Delta\Delta Ct}$ formula.[23] Statistical significance was assessed via Student's *t*-test.

Statistical analysis

Quantitative analysis was carried out using ImageJ software and GraphPad Prism version 8.0.0 for Windows (GraphPad Software, Boston, MA, USA, www.graphpad.com), with a sample size of 6. The results are reported as the mean ± standard deviation. Student's *t*-test was used to determine significant differences between the two groups ($\alpha = 0.05$), using IBM SPSS Statistics for Macintosh, Version 23.0 (IBM Corporation, Armonk, NY, USA).

Results

Confirmation of osteoarthritic changes in TMJ

Histological and immunohistochemical examinations were conducted to delineate the features of the TMJ OA model (**Figure 1**). Compared with the control group, safranin O-positive area in condyles showed a significant reduction in the UAC group ($P < 0.05$), indicating that UAC-induced TMJ OA resulted in glycosaminoglycan degradation in cartilage (**Figure 1A**). Further, as shown in **Figure 1B**, the amount of subchondral bone blood vessels during OA progression was significantly increased, while the UAC group showed significantly lower BV/TV on bone histomorphometry ($P < 0.05$). These observations were consistent with the micro-computed tomography derived data, corroborating a diminished BV/TV in the UAC group (**Figure 1C**), thus reinforcing the

validity of our findings on osteoarthritic changes. To examine changes in the distribution of nerve fibres, blood vessels, and inflammatory infiltration, immunofluorescence staining was executed to quantify the expression levels of CGRP, CD31, and CD4 (**Figure 1D**). We found increased distribution of nerve fibres, blood vessels, and immune cells in subchondral bone ($P < 0.05$), and they broke through tide mark and infiltrated into the condylar cartilage in the TMJ OA model. These findings indicate that UAC-induced TMJ OA model was successfully established.

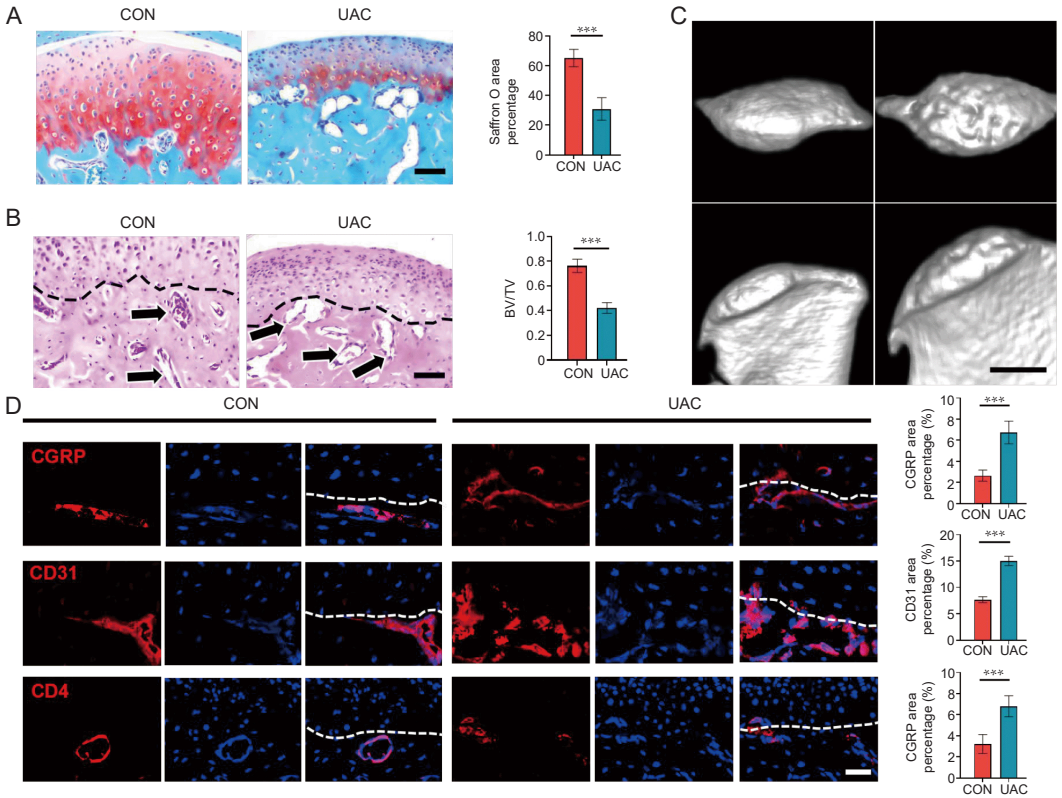

Figure 1. Histochemical and immunofluorescence staining of osteoarthritic changes in TMJ. (A, B) Representative images and corresponding statistical results of safranin O/fast green staining and HEstaining of mice TMJ in the CON and UAC groups. Arrows indicate the capillaries in subchondral bone. (C) Micro-computed tomography image of TMJ mice in the CON and UAC groups. (D) Comparison of CGRP, CD31, and CD4 expression levels in condylar subchondral bones between the groups. The white line represents the border between the cartilage and subchondral bone. CGRP indicated the distribution of nerve fibres and CD31 indicated that of blood vessels. Scale bars: 70 μm (A, B), 1 cm (C), 15 μm (D). Values are represented as mean ± SD ($n = 6$/group). ***$P < 0.001$ (Student's t-test). BV/TV: bone volume/tissue volume; CGRP: calcitonin gene-related peptide; CON: control; HE: haematoxylin–eosin; TMJ: temporomandibular joint; UAC: unilateral anterior crossbite.

Differential gene expression in subchondral bone

To further explore the differences between Control group and UAC group, we conducted whole mouse genome microarray. The microarray identified 41,175 genes. After applying rigorous statistical filters, specifically demanding fold change ≥ 2, and $P < 0.05$, we identified a cohort of 168 genes that were significantly upregulated and 14 genes that were notably downregulated, thereby elucidating a detailed transcriptional landscape. Inflammation- and angiogenesis-related DEGs are listed in **Additional Tables 2** and **3**, respectively.

The correlation plot in **Figure 2A** reveals a striking divergence in the gene expression at the genome-wide level, evidencing distinct patterns between the control and UAC groups. The volcano plot and heatmap show fold changes of all 182 DEGs expressed by subchondral bone in the UAC group relative to controls (**Figure 2B** and **C**). Preliminary examination of the microarray data disclosed the presence of DEGs. Nevertheless, the intricate interconnections between these genes and their specific roles in promoting disease progression are yet to be fully elucidated.

Enrichment analysis DEGs in subchondral bone

To further explore the detailed information pertaining to correlated pathways and their potential functions, GO and KEGG pathway enrichment analyses were performed with inflammation- (**Figure 3**), angiogenesis- (**Figure 4**), and neurogenesis-related genes (**Additional Figure 1**). All enrichment analysis plots were presented in the order of enriched factor. GO analysis uncovered enrichments in inflammation genes for T cell activation, lymphocyte aggregation, and regulation of T cell differentiation (**Figure 3A**), and in angiogenesis genes for regulation of angiogenesis,

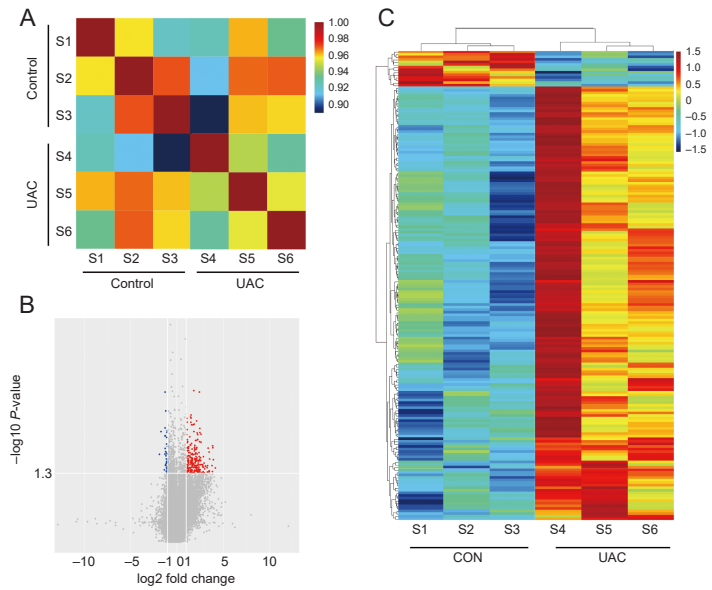

Figure 2. Transcriptomic analysis of DEGs in subchondral bone. (A) Correlation analysis with samples from the Control and UAC groups. (B) Volcano plot representation of gene expression analysis, highlighting the most affected DEGs. Red represents upregulated DEGs and blue represents downregulated DEGs. (C) Heatmap showing integrated analyses of DEGs. *X*-axis: Group clustering; *Y*-axis: Gene clustering. Red and blue indicate upregulated DEGs and downregulated DEGs, respectively; yellow, no change. Colour intensity reflects gene expression significance. CON: control; DEG: differentially expressed gene; S1–6: samples 1–6; UAC: unilateral anterior crossbite.

angiogenesis, and vasculature development (**Figure 4A**). KEGG analysis identified the mammalian target of rapamycin (mTOR)/nuclear factor-κB (NF-κB)/tumour necrosis factor (TNF) pathways for inflammation (**Figure 3B**), and phosphoinositide 3-kinase (PI3K)-protein kinase B (AKT)/vascular endothelial growth factor (VEGF)/hypoxia-inducible factor 1 (HIF-1) pathways for angiogenesis (**Figure 4B**). These findings confirm the significant role of immunological and vascular changes in the pathogenesis of TMJ OA.

PPI network analysis

To explore hub genes (genes with high correlation in candidate modules), the STRING database was used for PPI analysis. Inflammation- (**Figure 5A**) and angiogenesis-related genes (**Figure 5B**) were analysed separately. Cytoscape was used to understand the relationship among all selected genes (**Figure 5C**). The following related genes were identified: *Cd19*, *Cxcr4*, *Pi3kcd*, *Cd79a*, TNF receptor superfamily member 13b (*Tnfrsf13b*) and 13c (*Tnfrsf13c*), *Cd79b*, *Camp*, *Myb*, and Spi-B transcription factor (*Spib*). *Pi3kcd*, *Cxcr4*, *Camp*, and *Myb* were remarkably involved in both inflammation and angiogenesis. In particular, Pi3kcd participated in several activities, such as axon guidance, VEGF signalling pathway, and T cell receptor signalling pathway.

qPCR verification

In order to verify the accuracy of the microarray results, we conducted validation using qPCR. Four inflammation and angiogenesis-related genes: *Pi3kcd*, *Camp*, *Cxcr4*, and *Myb*, were validated (**Figure 6**). Consistent expression patterns of the selected genes were observed across both qPCR and microarray analyses, confirming the concordance of the data. Thus, qPCR results substantiated the veracity of the microarray data, reinforcing evidence for altered expression profiles in inflammation- and angiogenesis-associated genes within the subchondral bone of murine TMJ OA.

Discussion

Both abnormal remodelling of subchondral bone and joint pain occurs at the early stage of OA and aggravates as the disease progress, indicating that a potential pathogenic relationship exists between subchondral bone pathology and pain occurrence. In this study, we established a TMJ OA mouse model characterised by a heightened innervation and vascularisation of the subchondral bone, to identify predominant changes and pertinent signalling interactions within subchondral bone of osteoarthritic joints.

Through microarray-based transcriptomic profiling, we successfully discerned 182 DEGs that distinguished the Control group from the UAC group. Enrichment analyses of the DEGs revealed inflammation and angiogenesis as the paramount pathological changes. PPI analysis revealed a close interaction between inflammation- and angiogenesis-related DEGs, and several sub genes, such as *Pi3kcd*, *Camp*, *Cxcr4*, and *Myb* were found to serve as pivotal mediators in the intricate interplay between inflammation and angiogenesis. Considering that both inflammation and angiogenesis are pivotal in inducing ostealgia,[24] herein we demonstrated for the first time that signal interaction between inflammation and angiogenesis in TMJ osteoarthritic subchondral bone is closely interrelated and seems to play a vital role in the peripheral origin of OA pain.

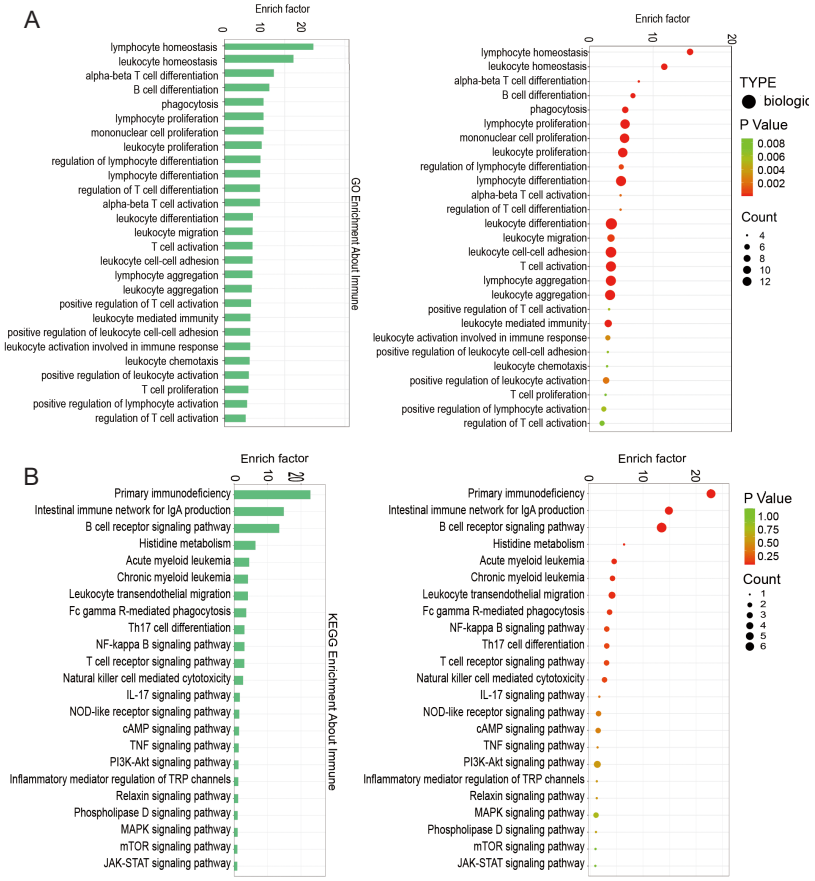

Figure 3. Functional enrichment analyses of DEGs associated with inflammation. (A) GO term categorisation. (B) KEGG pathway mapping. DEG: differentially expressed gene; GO: Gene Ontology; KEGG: Kyoto Encyclopedia of Genes and Genomes.

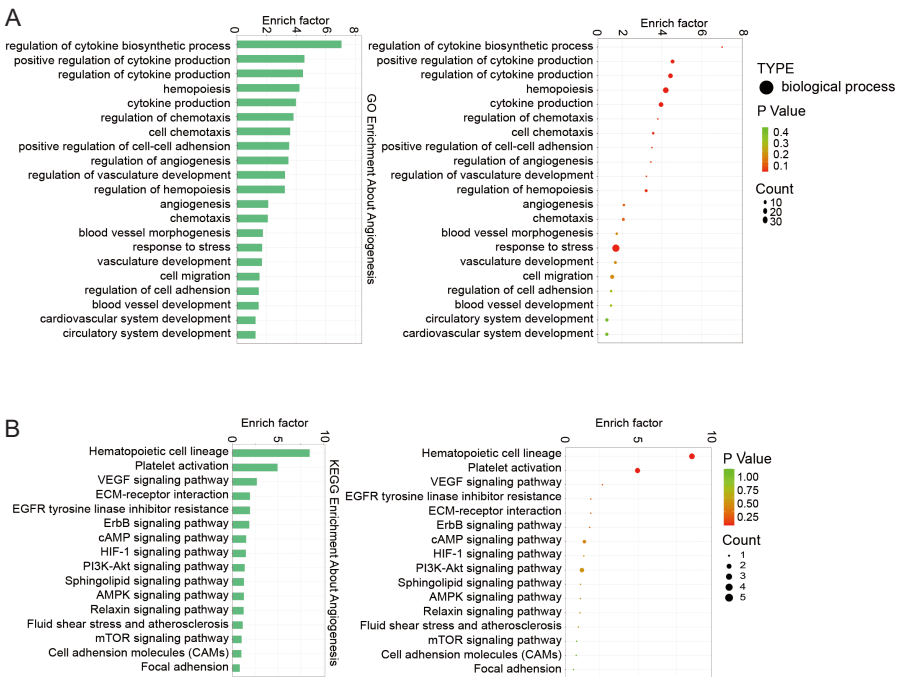

Figure 4. Functional enrichment analyses of DEGs associated with angiogenesis. (A) GO term categorisation. (B) KEGG pathway mapping. DEG: differentially expressed gene; GO: Gene Ontology; KEGG: Kyoto Encyclopedia of Genes and Genomes.

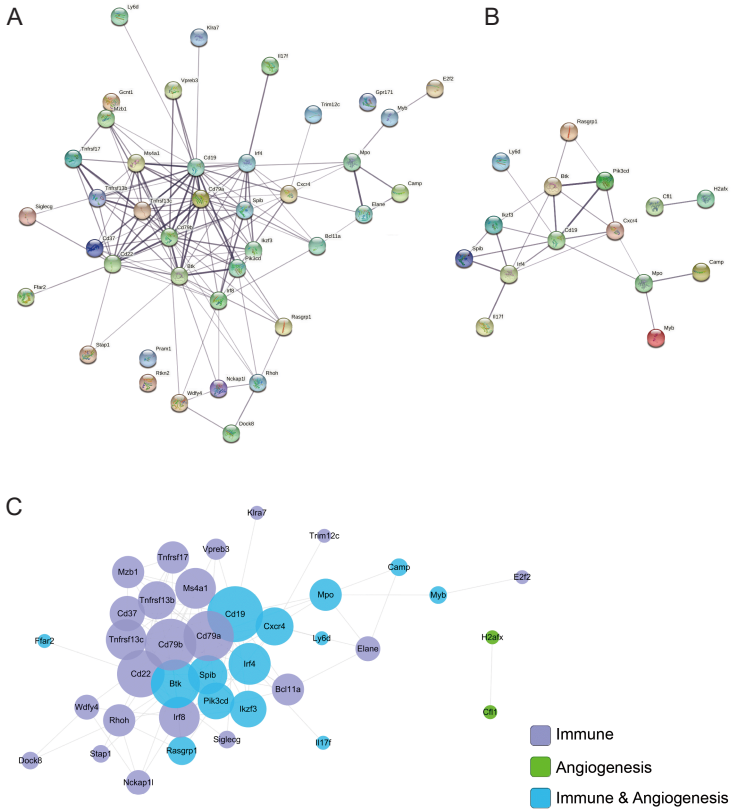

Figure 5. Protein–protein interaction (PPI) analysis. (A) Inflammation PPI network constructed with STRING. (B) Angiogenesis PPI network constructed with STRING. (C) Integrated PPI network visualised with Cytoscape.

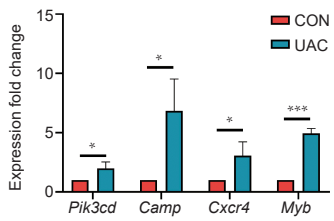

Figure 6. Gene expression of *Pi3kcd*, *Cxcr4*, *Camp*, and *Myb* under qPCR verification. Values are represented as mean ± SD (n = 6/group). *P < 0.05, ***P < 0.001 (Student's t-test). Camp: cathelicidin antimicrobial peptide; CON: contrtol; Cxcr4: C-X-C motif chemokine receptor 4; Myb: MYB proto-oncogene transcription factor; Pi3kcd: phosphatidylinositol-4,5-bisphosphate 3-kinase catalytic subunit delta; qPCR: quantitative polymerase chain reaction; UAC: unilateral anterior crossbite.

GO enrichment analysis disclosed a remarkable overrepresentation of DEGs in the regulation of T cell activation and differentiation, underscoring their significance in orchestrating immune responses. T cell activation is intimately intertwined with the manifestation of pain symptoms; empirical evidence suggests that mice lacking T cells can not feel pain when experiencing traumatic nerve pain and that they regain the sensation of pain when reconstituted with CD4$^+$ T cells.[25] Pro-inflammatory mediators secreted by CD4$^+$ T cells participate in the association between T cells and pain.[26]

The KEGG pathway enrichment study uncovered a substantial enrichment of DEGs in the mTOR/NF-κB/TNF signalling cascades. The mTOR has been identified as a pivotal integrator of diverse cellular functions, notably lymphocyte proliferation and activation in the context of tissue injury responses.[27,28] NF-κB signalling occupies a cardinal position in mediating tissue damage in osteoarthritic joints as its involved in oxidative stress-activated processes and inflammatory response.[29] Besides, TNF-α accelerates the inflammatory progression of OA via NF-κB, drives inflammatory pain by activating macrophages, and stimulates osteoclasts.[30] Hence, our data cumulatively imply a pivotal role for neuroimmune crosstalk in the initiation and progression of chronic pain in TMJ OA. Our results concur with the findings of a recent meta-analysis which also reported changes in inflammation and emphasized their role in osteoarthritic joints.[11] Targeting these interactions may open a new window for curing OA pain.

Blood vessels originating from subchondral bone break through tide mark and infiltrate into cartilage in condyle with OA, with local upregulation of the expression of several factors in the microenvironment, such as VEGF, platelet-derived growth factor, and matrix metalloprotease-9.[31] This investigation uncovered elevated expression levels of pro-angiogenic factors in the subchondral bone microenvironment of osteoarthritic joints. KEGG pathway enrichment analysis highlighted a substantial enrichment of DEGs in VEGF/HIF-1/PI3K-Akt signalling pathways. These pathways influence each other and eventually promote type H vessel formation and vascularisation in the osteochondral junction.[32] Type H blood vessels exacerbate subchondral bone remodelling processes, facilitating sensory nerve ingrowth within the subchondral bone compartment and thereby amplifying pain hypersensitivity in OA.[33] Our data substantiate that angiogenesis can lead to pain in patients with OA, probably by facilitating inflammation and enabling innervation of joint tissues.

Immunity and angiogenesis closely interact with each other and also evidently share regulatory pathways; moreover, they contribute to the structural deterioration and heightened pain sensations characteristic of OA. Thus, targeting and intercepting these intricate interactions may open novel therapeutic avenues for alleviating pain in OA. We found *Pi3kcd* expression to be upregulated in osteoarthritic subchondral bone, in accordance with a study on peripheral blood monocyte gene expression signatures in OA.[34] PI3KCD promotes the progression of OA in several cell types, such as osteoclast,[34] fibroblast-like synoviocytes,[35] and chondrocytes.[36] Through the PI3K-AKT/mechanistic target of rapamycin complex 1 (mTORC1) pathway, CXCL12 (aka stromal cell-derived factor-1) secretion increases in lymphocytes, which involves interactions with CXCR4 to aggravate bone lesions.[37] Besides, mTORC1 produced via this pathway involves the translation of VEGF, which eventually promotes angiogenesis.[38] On suppression of PI3K-AKT signalling via the pharmacological inhibitor LY294002, the function of osteoclasts is inhibited,[39] which eventually inhibiting subchondral bone resorption and osteoarthritic pain. We also found that *Cxcr4* expression was upregulated in osteoarthritic subchondral bone. CXCR4 is a 7-transmembrane G-protein-coupled receptor for chemokines and regulates diverse homeostatic processes, including inflammation, angiogenesis, and neurogenesis, during chronic diseases, such as OA.[40] CXCR4 works with its ligand CXCL12 to maintain tissue homeostasis and traffic immune cells. On the binding of CXCL12 to CXCR4, the conformation of transforming growth factor-β receptor type I changes, cells are activated, and diverse cytokines, including VEGF, are released, which promotes angiogenesis and inflammation in OA.[41] Once CXCL12/CXCR4 activity is inhibited, for example, by miRNA-140-3p,[42] OA progression is rescued. Notably, Furthermore, an upregulation in Camp expression was observed, implicating heightened activity of its bioactive product, LL-37 — a 37-amino acid peptide, can modulate cytokines released from different immune cells and angiogenesis.[43] Furthermore, it binds to formyl peptide receptor-like 1 expressed on endothelial cells to induce angiogenesis and acts on myeloid cells to promote the release of cytokines, such as interleukin-8 and -1β.[44] Inflammation stimulates angiogenesis, and angiogenesis facilitates inflammation. Individualised therapies targeting angiogenesis,[45, 46] pain, or inflammation[47, 48] alleviate OA symptoms; however, therapies that integrate modulation of inflammation-angiogenesis-neurogenesis crosstalk are imperative for optimizing treatment efficacy.

This study has several limitations. Compared with other gene expression profiles, our data may have some differences not completely match other data, which could be attributed to differences in modeling methods and different disease stages and severity. The other limitation is related to the development of scientific technology. New technologies, ranging from single-cell and single-nucleus RNA sequencing methods to spatial transcriptomics, have become much more popular and can generate a lot more data than microarray. Future studies should apply high-throughput sequencing to more comprehensively explore TMJ OA.

To conclude, signal transduction was found to be interrelated between inflammation (mTOR/NF-κB/TNF signalling) and angiogenesis (PI3K-Akt/VEGF/HIF-1 signalling) in osteoarthritic subchondral bone. *Pi3kcd*, *Camp*, *Cxcr4*, and *Myb* seem to play important roles in this interaction. Therefore, regulating the subchondral microenvironment may pave the way for advanced OA therapeutics.

Author contributions

Conceptualisation, manuscript draft, and visualisation: WQ, JG, JY; Methodolog and resources: WQ, JG, JY, XH, WL, ZM; manuscript review & editing: WQ, JG, JY, LN, KJ; supervision, and project administration: LN, KJ; funding acquisition: KJ. All authors read and approved the final version of the manuscript.

Financial support

This work was supported by the National Key Research and development Programme, No. 2023YFC2509100, National Natural Science Foundation of China, No. 82170978, and Distinguished Young Scientists Funds of Shaanxi Province, No. 2021JC-34 (all to JK).

Acknowledgement

The authors thank the State Key Laboratory of Military Stomatology, National Clinical Research Centre for Oral Diseases, School of Stomatology, The Fourth Military Medical University for providing us with the experimental platform and scientific research instruments.

Conflicts of interest statement

The authors declared no potential conflict of interest with respect to the research, authorship, and/or publication of this work.

Additional files

Additional Table 1: Primer sequences used for quantitative real-time polymerase chain reaction in the present study.

Additional Table 2: Representative differentially expressed genes with known or suspected roles in inflammation.

Additional Table 3: Representative differentially expressed genes with known or suspected roles in angiogenesis.

Additional Figure 1: Functional enrichment analyses of DEGs associated with neurogenesis.

1. Wen, C.; Xiao, G. Advances in osteoarthritis research in 2021 and beyond. *J Orthop Translat.* **2022**, *32*, A1-A2.

2. Yao, Q.; Wu, X.; Tao, C.; Gong, W.; Chen, M.; Qu, M.; Zhong, Y.; He, T.; Chen, S.; Xiao, G. Osteoarthritis: pathogenic signaling pathways and therapeutic targets. *Signal Transduct Target Ther.* **2023**, *8*, 56.
3. Lluch, E.; Torres, R.; Nijs, J.; Van Oosterwijck, J. Evidence for central sensitization in patients with osteoarthritis pain: a systematic literature review. *Eur J Pain.* **2014**, *18*, 1367-1375.
4. Cohen, E.; Lee, Y. C. A mechanism-based approach to the management of osteoarthritis pain. *Curr Osteoporos Rep.* **2015**, *13*, 399-406.
5. Mathiessen, A.; Conaghan, P. G. Synovitis in osteoarthritis: current understanding with therapeutic implications. *Arthritis Res Ther.* **2017**, *19*, 18.
6. Sun, Q.; Zhen, G.; Li, T. P.; Guo, Q.; Li, Y.; Su, W.; Xue, P.; Wang, X.; Wan, M.; Guan, Y.; Dong, X.; Li, S.; Cai, M.; Cao, X. Parathyroid hormone attenuates osteoarthritis pain by remodeling subchondral bone in mice. *Elife.* **2021**, *10*, e66532.
7. de Castro, J. C.; Henares-Esguerra, E. L.; Olivia, S. T. S. M. B.; Wang, D.; Chang Chien, G. C. Photoactivated leucocyte-rich platelet-rich plasma treatment in reduction of bone marrow edema in hip osteoarthritis. *Regen Med.* **2022**, *17*, 521-531.
8. Laslett, L. L.; Doré, D. A.; Quinn, S. J.; Boon, P.; Ryan, E.; Winzenberg, T. M.; Jones, G. Zoledronic acid reduces knee pain and bone marrow lesions over 1 year: a randomised controlled trial. *Ann Rheum Dis.* **2012**, *71*, 1322-1328.
9. Isaac, D.; Falode, T.; Liu, P.; I'Anson, H.; Dillow, K.; Gill, P. Accelerated rehabilitation after total knee replacement. *Knee.* **2005**, *12*, 346-350.
10. Zhu, S.; Zhu, J.; Zhen, G.; Hu, Y.; An, S.; Li, Y.; Zheng, Q.; Chen, Z.; Yang, Y.; Wan, M.; Skolasky, R. L.; Cao, Y.; Wu, T.; Gao, B.; Yang, M.; Gao, M.; Kuliwaba, J.; Ni, S.; Wang, L.; Wu, C.; Findlay, D.; Eltzschig, H. K.; Ouyang, H. W.; Crane, J.; Zhou, F. Q.; Guan, Y.; Dong, X.; Cao, X. Subchondral bone osteoclasts induce sensory innervation and osteoarthritis pain. *J Clin Invest.* **2019**, *129*, 1076-1093.
11. Boer, C. G.; Hatzikotoulas, K.; Southam, L.; Stefánsdóttir, L.; Zhang, Y.; Coutinho de Almeida, R.; Wu, T. T.; Zheng, J.; Hartley, A.; Teder-Laving, M.; Skogholt, A. H.; Terao, C.; Zengini, E.; Alexiadis, G.; Barysenka, A.; Bjornsdottir, G.; Gabrielsen, M. E.; Gilly, A.; Ingvarsson, T.; Johnsen, M. B.; Jonsson, H.; Kloppenburg, M.; Luetge, A.; Lund, S. H.; Mägi, R.; Mangino, M.; Nelissen, R.; Shivakumar, M.; Steinberg, J.; Takuwa, H.; Thomas, L. F.; Tuerlings, M.; Babis, G. C.; Cheung, J. P. Y.; Kang, J. H.; Kraft, P.; Lietman, S. A.; Samartzis, D.; Slagboom, P. E.; Stefansson, K.; Thorsteinsdottir, U.; Tobias, J. H.; Uitterlinden, A. G.; Winsvold, B.; Zwart, J. A.; Davey Smith, G.; Sham, P. C.; Thorleifsson, G.; Gaunt, T. R.; Morris, A. P.; Valdes, A. M.; Tsezou, A.; Cheah, K. S. E.; Ikegawa, S.; Hveem, K.; Esko, T.; Wilkinson, J. M.; Meulenbelt, I.; Lee, M. T. M.; van Meurs, J. B. J.; Styrkársdóttir, U.; Zeggini, E. Deciphering osteoarthritis genetics across 826,690 individuals from 9 populations. *Cell.* **2021**, *184*, 4784-4818.e17.
12. Jiang, W.; Jin, Y.; Zhang, S.; Ding, Y.; Huo, K.; Yang, J.; Zhao, L.; Nian, B.; Zhong, T. P.; Lu, W.; Zhang, H.; Cao, X.; Shah, K. M.; Wang, N.; Liu, M.; Luo, J. PGE2 activates EP4 in subchondral bone osteoclasts to regulate osteoarthritis. *Bone Res.* **2022**, *10*, 27.
13. Kalladka, M.; Young, A.; Thomas, D.; Heir, G. M.; Quek, S. Y. P.; Khan, J. The relation of temporomandibular disorders and dental occlusion: a narrative review. *Quintessence Int.* **2022**, *53*, 450-459.
14. Sun, J. L.; Yan, J. F.; Li, J.; Wang, W. R.; Yu, S. B.; Zhang, H. Y.; Huang, F.; Niu, L. N.; Jiao, K. Conditional deletion of Adrb2 in mesenchymal stem cells attenuates osteoarthritis-like defects in temporomandibular joint. *Bone.* **2020**, *133*, 115229.
15. Qin, W.; Zhang, Z.; Yan, J.; Han, X.; Niu, L. N.; Jiao, K. Interaction of neurovascular signals in the degraded condylar cartilage. *Front Bioeng Biotechnol.* **2022**, *10*, 901749.
16. Ye, T.; Sun, D.; Mu, T.; Chu, Y.; Miao, H.; Zhang, M.; Yang, H.; Liu, Q.; Lu, L.; Xing, X.; Yu, S. Differential effects of high-physiological oestrogen on the degeneration of mandibular condylar cartilage and subchondral bone. *Bone.* **2018**, *111*, 9-22.
17. Jiao, K.; Dai, J.; Wang, M. Q.; Niu, L. N.; Yu, S. B.; Liu, X. D. Age- and sex-related changes of mandibular condylar cartilage and subchondral bone: a histomorphometric and micro-CT study in rats. *Arch Oral Biol.* **2010**, *55*, 155-163.
18. Kanehisa, M.; Sato, Y.; Furumichi, M.; Morishima, K.; Tanabe, M. New approach for understanding genome variations in KEGG. *Nucleic Acids Res.* **2019**, *47*, D590-D595.
19. Szklarczyk, D.; Gable, A. L.; Lyon, D.; Junge, A.; Wyder, S.; Huerta-Cepas, J.; Simonovic, M.; Doncheva, N. T.; Morris, J. H.; Bork, P.; Jensen, L. J.; Mering, C. V. STRING v11: protein-protein association networks with increased coverage, supporting functional discovery in genome-wide experimental datasets. *Nucleic Acids Res.* **2019**, *47*, D607-D613.
20. Shannon, P.; Markiel, A.; Ozier, O.; Baliga, N. S.; Wang, J. T.; Ramage, D.; Amin, N.; Schwikowski, B.; Ideker, T. Cytoscape: a software environment for integrated models of biomolecular interaction networks. *Genome Res.* **2003**, *13*, 2498-2504.
21. Yan, J.; Shen, M.; Sui, B.; Lu, W.; Han, X.; Wan, Q.; Liu, Y.; Kang, J.; Qin, W.; Zhang, Z.; Chen, D.; Cao, Y.; Ying, S.; Tay, F. R.; Niu, L. N.; Jiao, K. Autophagic LC3(+) calcified extracellular vesicles initiate cartilage calcification in osteoarthritis. *Sci Adv.* **2022**, *8*, eabn1556.
22. Qin, W. P.; Wan, Q. Q.; Yan, J. F.; Han, X. X.; Lu, W. C.; Ma, Z. Y.; Ye, T.; Li, Y. T.; Li, C. J.; Wang, C.; Tay, F. R.; Niu, L. N.; Jiao, K. Effect of Extracellular Ribonucleic Acids on Neurovascularization in Osteoarthritis. *Adv Sci (Weinh).* **2023**, *10*, e2301763.
23. Livak, K. J.; Schmittgen, T. D. Analysis of relative gene expression data using real-time quantitative PCR and the 2(-Delta Delta C(T)) method. *Methods.* **2001**, *25*, 402-408.
24. Bonnet, C. S.; Walsh, D. A. Osteoarthritis, angiogenesis and inflammation. *Rheumatology (Oxford).* **2005**, *44*, 7-16.
25. Kavelaars, A.; Heijnen, C. J. T cells as guardians of pain resolution. *Trends Mol Med.* **2021**, *27*, 302-313.
26. Kavelaars, A.; Heijnen, C. J. Immune regulation of pain: friend and foe. *Sci Transl Med.* **2021**, *13*, eabj7152.
27. Iwata, T. N.; Ramírez-Komo, J. A.; Park, H.; Iritani, B. M. Control of B lymphocyte development and functions by the mTOR signaling pathways. *Cytokine Growth Factor Rev.* **2017**, *35*, 47-62.
28. Suto, T.; Karonitsch, T. The immunobiology of mTOR in autoimmunity. *J Autoimmun.* **2020**, *110*, 102373.
29. Lepetsos, P.; Papavassiliou, K. A.; Papavassiliou, A. G. Redox and NF-κB signaling in osteoarthritis. *Free Radic Biol Med.* **2019**, *132*, 90-100.
30. Baral, P.; Udit, S.; Chiu, I. M. Pain and immunity: implications for host defence. *Nat Rev Immunol.* **2019**, *19*, 433-447.
31. Hu, Y.; Chen, X.; Wang, S.; Jing, Y.; Su, J. Subchondral bone microenvironment in osteoarthritis and pain. *Bone Res.* **2021**, *9*, 20.
32. Fernández-Torres, J.; Zamudio-Cuevas, Y.; Martínez-Nava, G. A.; López-Reyes, A. G. Hypoxia-inducible factors (HIFs) in the articular cartilage: a systematic review. *Eur Rev Med Pharmacol Sci.* **2017**, *21*, 2800-2810.
33. Peng, Y.; Wu, S.; Li, Y.; Crane, J. L. Type H blood vessels in bone modeling and remodeling. *Theranostics.* **2020**, *10*, 426-436.
34. Shi, T.; Shen, X.; Gao, G. Gene expression profiles of peripheral blood

monocytes in osteoarthritis and analysis of differentially expressed genes. *Biomed Res Int.* **2019**, *2019*, 4291689.
35. Bartok, B.; Hammaker, D.; Firestein, G. S. Phosphoinositide 3-kinase δ regulates migration and invasion of synoviocytes in rheumatoid arthritis. *J Immunol.* **2014**, *192*, 2063-2070.
36. Yamaguchi, Y.; Kanzaki, H.; Miyamoto, Y.; Itohiya, K.; Fukaya, S.; Katsumata, Y.; Nakamura, Y. Nutritional supplementation with myo-inositol in growing mice specifically augments mandibular endochondral growth. *Bone.* **2019**, *121*, 181-190.
37. Sun, K.; Luo, J.; Guo, J.; Yao, X.; Jing, X.; Guo, F. The PI3K/AKT/mTOR signaling pathway in osteoarthritis: a narrative review. *Osteoarthritis Cartilage.* **2020**, *28*, 400-409.
38. Ding, W.; Chen, X.; Yang, L.; Chen, Y.; Song, J.; Bu, W.; Feng, B.; Zhang, M.; Luo, Y.; Jia, X.; Feng, L. Combination of ShuangDan capsule and sorafenib inhibits tumor growth and angiogenesis in hepatocellular carcinoma via PI3K/Akt/mTORC1 pathway. *Integr Cancer Ther.* **2022**, *21*, 15347354221078888.
39. Cao, H.; Zhu, K.; Qiu, L.; Li, S.; Niu, H.; Hao, M.; Yang, S.; Zhao, Z.; Lai, Y.; Anderson, J. L.; Fan, J.; Im, H. J.; Chen, D.; Roodman, G. D.; Xiao, G. Critical role of AKT protein in myeloma-induced osteoclast formation and osteolysis. *J Biol Chem.* **2013**, *288*, 30399-30410.
40. Pozzobon, T.; Goldoni, G.; Viola, A.; Molon, B. CXCR4 signaling in health and disease. *Immunol Lett.* **2016**, *177*, 6-15.
41. Qin, H. J.; Xu, T.; Wu, H. T.; Yao, Z. L.; Hou, Y. L.; Xie, Y. H.; Su, J. W.; Cheng, C. Y.; Yang, K. F.; Zhang, X. R.; Chai, Y.; Yu, B.; Cui, Z. SDF-1/CXCR4 axis coordinates crosstalk between subchondral bone and articular cartilage in osteoarthritis pathogenesis. *Bone.* **2019**, *125*, 140-150.
42. Ren, T.; Wei, P.; Song, Q.; Ye, Z.; Wang, Y.; Huang, L. MiR-140-3p ameliorates the progression of osteoarthritis via targeting CXCR4. *Biol Pharm Bull.* **2020**, *43*, 810-816.
43. Chen, X.; Qi, G.; Qin, M.; Zou, Y.; Zhong, K.; Tang, Y.; Guo, Y.; Jiang, X.; Liang, L.; Zou, X. DNA methylation directly downregulates human cathelicidin antimicrobial peptide gene (CAMP) promoter activity. *Oncotarget.* **2017**, *8*, 27943-27952.
44. Bucki, R.; Leszczyńska, K.; Namiot, A.; Sokołowski, W. Cathelicidin LL-37: a multitask antimicrobial peptide. *Arch Immunol Ther Exp (Warsz).* **2010**, *58*, 15-25.
45. Li, Y.; Mu, W.; Xu, B.; Ren, J.; Wahafu, T.; Wuermanbieke, S.; Ma, H.; Gao, H.; Liu, Y.; Zhang, K.; Amat, A.; Cao, L. Artesunate, an anti-malaria agent, attenuates experimental osteoarthritis by inhibiting bone resorption and CD31(hi)Emcn(hi) vessel formation in subchondral bone. *Front Pharmacol.* **2019**, *10*, 685.
46. Yajun, W.; Jin, C.; Zhengrong, G.; Chao, F.; Yan, H.; Weizong, W.; Xiaoqun, L.; Qirong, Z.; Huiwen, C.; Hao, Z.; Jiawei, G.; Xinchen, Z.; Shihao, S.; Sicheng, W.; Xiao, C.; Jiacan, S. Betaine attenuates osteoarthritis by inhibiting osteoclastogenesis and angiogenesis in subchondral bone. *Front Pharmacol.* **2021**, *12*, 723988.
47. Bhalekar, M. R.; Upadhaya, P. G.; Madgulkar, A. R. Fabrication and efficacy evaluation of chloroquine nanoparticles in CFA-induced arthritic rats using TNF-α ELISA. *Eur J Pharm Sci.* **2016**, *84*, 1-8.
48. Lee, H.; Lee, M. Y.; Bhang, S. H.; Kim, B. S.; Kim, Y. S.; Ju, J. H.; Kim, K. S.; Hahn, S. K. Hyaluronate-gold nanoparticle/tocilizumab complex for the treatment of rheumatoid arthritis. *ACS Nano.* **2014**, *8*, 4790-4798.

Received: April 15, 2024
Revised: May 21, 2024
Accepted: June 4, 2024
Available online: June 28, 2024